All-Organic Electrochromic Spandex

Michael A. Invernale, Yujie Ding, and Gregory A. Sotzing*

Department of Chemistry and the Polymer Program, University of Connecticut, 97 North Eagleville Road U-3136,
Storrs, Connecticut 06269-3136

ABSTRACT Herein we describe the preparation and characterization of reflective-type electrochromic devices using stretchable, conductive fabric electrodes. Two fabrics were used in this study: woven stainless steel mesh and Lycra spandex impregnated with a conducting polymer (poly[3,4-ethylenedioxythiophene]-poly[styrene sulfonate], PEDOT-PSS). Electrochromic polymers were prepared on the surface of these fabric electrodes and devices were assembled. The time taken for the electrochromic polymer to switch between colored states in devices prepared with stainless steel electrodes (conductivity ca. 9,800 S/cm) was ca. 0.3 s, whereas that using PEDOT-PSS loaded Lycra (conductivity ca. 0.1 S/cm) was a few seconds. The iris effect was evaluated for each of the device architectures, showing no effect for steel mesh/steel mesh devices and a propagating front for spandex-based devices. The electrochromic spandex functioned in solution while being stretched. In addition, stenciled devices were built. Such fabric electrochromic devices represent a critical step toward the realization of totally chameleonic fabric.

KEYWORDS: functional textile • spandex/fabric • electrochromic devices • organic electronics • electrochromic devices

INTRODUCTION

The applications for fabric electrochromics are vast, encompassing adaptive camouflage, biomimicry, wearable displays, and fashion. Such applications require many underlying and cooperative technologies. The work herein represents a necessary step toward the development of totally chameleonic fabric. The variety of color transitions, ease of processability, and stabilities afforded by conducting polymers make them desirable for flexible organic electronics. The fabric electrodes in these devices need not be highly conductive, allowing for use of a variety of conductive composites (1−7). Fabrics described herein demonstrate a red to blue color change, although any processable electrochromic material is feasible (8−18). Our efforts toward the development of processable conjugated polymers has made the reported fabric devices possible (19−22). Adaptive camouflage, chameleonic systems, and biomimicry have all been of great interest in the past. Fabric displays such as those developed herein comprise an enabling technology for fully wearable displays. Spandex could be ideal for biomimicry or chameleonic behavior in that color change can be triggered by an electrical response and color intensity modulated by stretching (23−30). Fabric has been used for color change applications in the past, however it was with photochromic dyes in textile (31−33). The ability to make the fabric electrochromic allows for user control over the color change. This control is a critical element for real-time adaptive technology.

Electrochromic devices (ECDs) have many compositions, usually with two conductive substrates sandwiching an electrochromic material and an electrolyte. Most transparent ECDs employ optically transparent electrodes consisting of indium-doped tin oxide (ITO) on glass or plastic. Reflective ECDs often use metallic working electrodes, such as gold, and ITO as the outer electrode (34, 35). Replacement of ITO with conducting polymers has been envisioned; PEDOT-PSS, having conductivities in the 100's of S/cm, was used as an electrode for ECDs and in organic photovoltaics (36−39). Electrochromic polymers have become increasingly processable as well, furthering the simplicity of ECD assembly. Our group's precursor polymer work involves synthesis of a soluble precursor polymer that can be converted to an electrochromic material after processing. These precursors can be patterned by methods such as spray-coating, inkjetting and e-spinning (19, 20). The precursor can then be oxidatively converted (electrochemically or chemically) to its electrochromic counterpart. A modified reflective-type device architecture was developed for the fabric ECDs (Figure 1).

RESULTS AND DISCUSSION

Conducting Fabric Properties.

Woven stainless steel mesh and PEDOT-PSS impregnated spandex were used as electrodes. The importance here is that for fabric electrochromic devices, ITO is not needed. The spandex is a commercially available material, Lycra, with a thread count of 5882 and 70.0 denier. The stainless steel has a thread count of 17 343 and 80.4 denier. The Lycra was soaked for 5 min in PEDOT-PSS (ORGACON S300) with 2 wt % *d*-sorbitol and allowed to air-dry. The resultant spandex electrode was electrochemically inert from −1.2 V to +2.0 V but functioned as an electrode to −2.0 V. The stainless steel mesh was electrochemically stable from −2.5 V to +1.8 V (vs Ag/Ag$^+$). Stainless steel has a conductivity of 9.8×10^3 S/cm, whereas the PEDOT-PSS soaked spandex is 7.7×10^{-2} S/cm, a 5 orders of magnitude difference. The spandex could still stretch up to 100% once it was soaked with the conducting polymer, while retaining a conductivity of 6.5×10^{-2} S/cm. Figure 1 shows a cross-sectional schematic of

---

* Corresponding author. Tel: (860) 486-4619. Fax: (860) 486-4745. E-mail: sotzing@mail.ims.uconn.edu.

Received for review November 5, 2009 and accepted December 17, 2009

DOI: 10.1021/am900767p

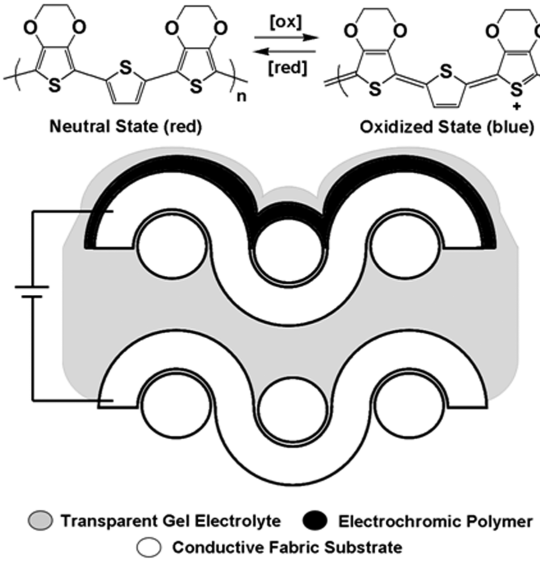

FIGURE 1. Schematic of the (top) EC polymer in each redox state; (bottom) fabric electrochromic device cross-section for a typical reflective device used in this study.

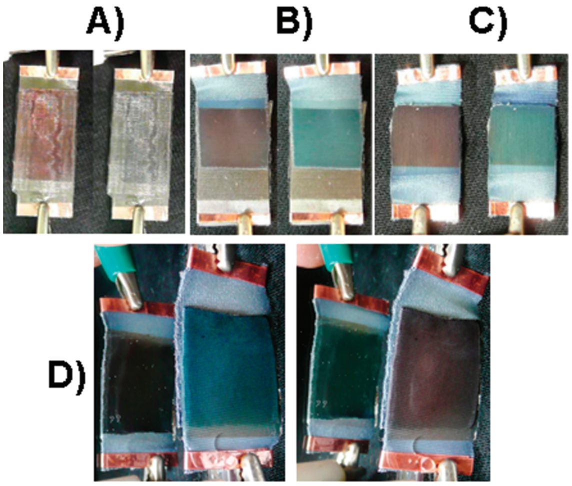

FIGURE 2. Images of fabric ECDs made with (A) two woven stainless steel substrates, (B) spandex working electrode and steel counter electrode, and (C) two spandex electrodes, in their oxidized (top) and neutral (bottom) states. (D) A two-sided device in positive (left) and negative (right) bias. This is one device placed in front of a mirror such that the color of each side of the fabric can be observed.

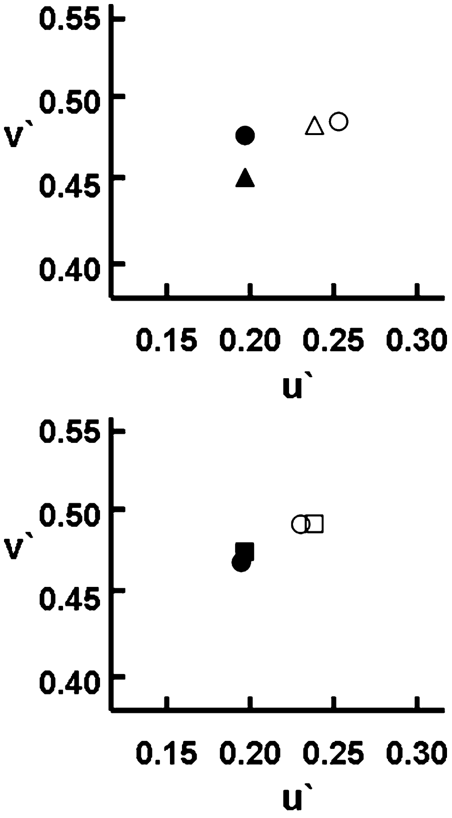

FIGURE 3. Colorimetry of fabric ECDs. (top) CIE Lu'v' color plot for steel (triangles) and spandex (circles) devices. Filled shapes represent the oxidized state; empty shapes represent the neutral state. (bottom) Comparison of stretched (circles) versus nonstretched (squares) fabric in each state. A color version of this figure appears in the Supporting Information.

the fabric electrochromic devices. Devices were assembled with steel as both electrodes, steel counter with spandex working electrode, and spandex as both electrodes.

Various Electrochromic Fabric Device Assembly. A reflective device was built by spray-casting the precursor onto one side of the steel or spandex. The precursor was converted at +1.1 V in a 0.1 M lithium triflate (LITRIF)/acetonitrile (ACN) electrolyte bath prior to assembly. The substrates were fused together using a photocurable gel electrolyte (poly(ethyleneglycol diacrylate), propylene carbonate, LITRIF, and photoinitiator). Two-sided devices, where the outer faces of both electrodes were coated with electrochromic material, were also made. When assembled together as working and counter, this produced a device which was simultaneously red on one side and blue on the other. Two different electrochromic polymers could thus be used to generate a four-color reversible fabric. Figure 2 shows images of these fabric ECDs.

Colorimetry. The difference in color, based upon the choice of electrode, was assessed using a colorimeter. The bare steel was found to have $L = 29.8$, $u' = 0.2052$, $v' = 0.4505$. The neutral state on stainless steel had values of $L = 15.5$, $u' = 0.2353$, $v' = 0.4815$ (standard deviation ± 0.0004) and the oxidized state was $L = 22.7$, $u' = 0.1990$, $v' = 0.4475$ (standard deviation ± 0.0005). For the spandex, the coordinates were $L = 30.3$, $u' = 0.1942$, $v' = 0.4808$. The neutral state on spandex had values of $L = 10.1$, $u' = 0.2446$, $v' = 0.4957$ (standard deviation ± 0.0015) and the oxidized state was $L = 11.3$, $u' = 0.2010$, $v' = 0.4864$ (standard deviation ± 0.0020). There was a clear effect of substrate on perceived color. The gray color of the steel mesh as compared to the light-blue color of the PEDOT-PSS spandex contributed to the observed variations, even though the electrochromic was the same. Stretching the spandex fabric did not cause a distortion of color. The colorimeter was focused on individual fiber bundles that were being stretched to 20% in each direction and that were unstretched; the color coordinates overlapped in each case. Figure 3 contains a plot of the CIE 1976 Lu'v' color coordinates for the stainless steel and spandex fabric devices, as well as the overlap between stretched and nonstretched samples.

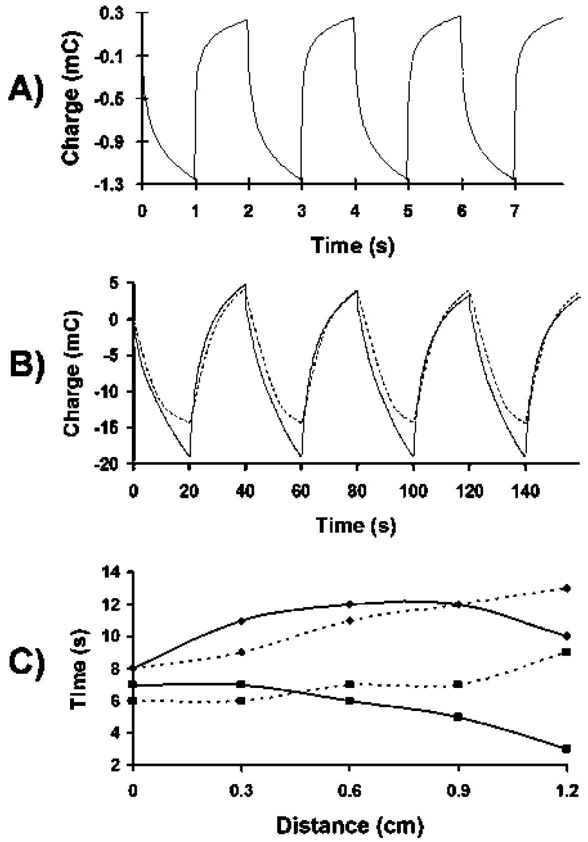

FIGURE 4. Chronocoulometry response between −2.0 V and +2.0 V (vs Ag/Ag$^+$) for devices whose working electrode/counter electrode configurations are (A) steel/steel and (B) spandex/steel (dashed line) overlaid with spandex/spandex (solid line). (C) Image analysis of switching time with respect to distance across the active area for oxidation (diamonds) and reduction (squares) of spandex/steel (solid lines) and spandex/spandex (dotted line) devices.

Switching Speed and the Iris Effect. Switching speeds of these devices were examined; the characteristics for steel devices were faster than those utilizing spandex. This result was expected, however a much larger gap in switch speed was anticipated considering the five-orders-of-magnitude difference in conductivities between the electrodes. Solution studies of the working electrodes were performed using a 0.1 M LITRIF/ACN electrolyte bath; 1.6 cm^2 area electrodes were used for solution studies and device fabrication; oxidation and reduction times were taken at 90% charge and were averaged over 4 samples. The steel accomplished a switch in 207 ± 12 ms in solution, whereas solid-state devices achieved a switch in 318 ± 33 ms. Solution switching for the spandex electrode occurred in 12.20 ± 0.15 s while the corresponding all-spandex device switched in 14.53 ± 0.53 s. Fabric devices prepared using a spandex working electrode with a steel counter electrode switched in 13.11 ± 0.14 s. Thus, there was no large effect of the counter electrode on response time. Diffusion is the limiting factor for electrochromic function, and though steel/steel devices performed faster than spandex/spandex ones, the spandex/steel device was not significantly affected by the change in counter electrode. Figure 4 shows the chronocoulometry for these devices, switched at potentials of −2.0 V to +2.0 V. In solution, the charge observed for a switching cycle on a spandex electrode was 49.11 mC, whereas the charge to switch the same mass of polymer on a stainless steel plate was 9.99 mC. The excess charge observed in the case of the fabric electrode can be attributed to the PEDOT-PSS (either directly or indirectly, via the charging current observed during the longer switching times).

The Iris Effect is a phenomenon that occurs for electrochromic devices that use a nonmetal conductor, such as ITO or PEDOT-PSS. It is a process by which the edges of a device switch faster than its center, resulting in an observable "iris." Charge propagation, and thus redox activity, across the device electrodes is responsible for the Iris Effect. In order to assess this process within our system, the optical kinetics of the solid-state fabric ECDs were evaluated with ImageJ software to analyze movies of these devices switching, taken at 25 frames per second. The software maps RGB coordinates with respect to time and distance. Distances over the active area of a device between leads (perpendicular) were divided evenly; data was analyzed at each point, including edges. This was the easiest way to obtain optical switching speeds to correlate with those calculated from chronocoulometric measurements. As is evidenced by the optical switching speeds (12.0 s to oxidize, 6 s to reduce for steel/spandex; 11.0 s to oxidize, 7 s to reduce for spandex/spandex), the optical switching speeds were faster than those calculated from the charge data for spandex devices. This can again be attributed to the charging effects observed for conducting spandex systems, as discussed previously.

According to image analysis, there was no observable iris effect for steel/steel devices on the time scale frames were taken. Figure 4C illustrates that there was an effect for spandex/steel and spandex/spandex devices, possibly attributed to the lower conductivity of the PEDOT-PSS. With the spandex/spandex device, the color change propagated as a front, beginning from one of the electrode leads and moving across the length of the device. whereas, the spandex/steel device demonstrated more of a traditional iris effect during oxidation; color changed first on the periphery and progressed inward as indicated by the curvature of the data. Further, the optical memory of both the spandex-based and steel-based devices, in both the oxidized and neutral states, was stable for more than 24 h, with no observable changes in color or oxidation state after these periods.

Performance While Being Stretched and Stenciled into Fabric Devices. The electrochromic states of a stretched electrode were also examined. Figure 5 shows the stretchable electrode in solution (0.1 M LITRIF/ACN). The spandex was stretched by 20% in each direction and was switched. The background can be seen through the porosity of the stretched fabric. Color density decreases upon stretching on the macroscale, but focusing on individual fibers produces overlapping color results on the microscale. The fabric electrode was still functional and the time necessary to achieve switching was within one standard deviation of the unstretched form. Showing its versatility, the precursor polymer was stencil-patterned onto PEDOT-PSS-loaded spandex and made into simple display devices (Figure 5). The

FIGURE 5. Images of (A) stretched, spandex fabric electrode in electrolyte bath switching an EC polymer from its neutral (left) to oxidized (right) states. (B) Stencil-patterned solid-state fabric ECD in its neutral (top) and oxidized (bottom) state.

color-change property of this stenciled logo lends itself to simple text displays incorporated into fabric.

CONCLUSIONS

We have made a requisite technological component of chameleonic fabric. The work herein represents a critical element for the realization of this application. The incorporation of new, flexible, stretchable conductive substrates into ECDs has been achieved. There is a 50-fold change in response time with a 100 000-fold difference in substrate conductivity. The spandex-based electrode switched between the same colors in the stretched and unstretched states while having the same response speeds, indicating the properties of the conductor, PEDOT-PSS, and the electrochromic remain intact. The ability of a fabric ECD to mold to a surface and for the device itself to stretch and contort are all essential components of chameleonic clothing, biomimicry, adaptive camouflage, wearable displays, and fashion-related applications. Work toward achieving such properties in a fully assembled device is underway, as well as electrochromic thread. Innumerable polymeric systems could be employed with these architectures, opening up a wide range of possibilities for the display and textile industries.

EXPERIMENTAL SECTION

Materials. Acetonitrile (ACN), *n*-pentane, tetrahydrofuran, and dichloromethane were purchased from Thermo-Fisher and distilled over calcium hydride before use. *n*-Butyl lithium (2.6 M in hexanes), lithium trifluoromethane sulfonate (LITRIF), propylene carbonate (PC), polyethylene glycol diacrylate (PEG-DA), and dimethoxyphenylacetophenone (DMPAP) were purchased from Sigma Aldrich and used as received. Dichlorodioctylsilane was purchased from Gelest Inc. and distilled prior to use. Copper tape was purchased from Newark. The metal mesh was a generous gift from ITP GmbH. The Lycra spandex was generously donated by Lubrizol. ORGACON S300 PEDOT-PSS dispersion was procured from Agfa. Sorbitol was purchased from Thermo-Fisher and used as received.

Electrochemistry. Electrochemical conversion of the precursor polymer to its conjugated, electrochromic form and chronocoulometry were carried out with a CHI 400A potentiostat. Conversions were carried out in 0.1 M LITRIF/ACN electrolyte solutions, with respect to a nonaqueous Ag/Ag$^+$ reference electrode, calibrated to 0.455 V vs NHE.

Device Assembly. Stainless steel mesh electrodes were used as-cut from larger woven sheets. The spandex electrodes were prepared by soaking the desired size electrode in 2 wt % d-sorbitol-doped PEDOT-PSS aqueous dispersion for 5 min. They were allowed to air-dry before use. A gel electrolyte comprising 1 g of LITRIF, 5 g of PC, 5 g of PEG-DA, and 18 mg of DMPAP was used for all devices (20). A 365 nm UV light compartment was used to cure the gel electrolyte. The substrates were spray-coated with precursor polymer from DCM using an Iwata spray coater and the precursor polymer was converted oxidatively in an electrolyte bath before use in device fabrication.

Optical Characterization. Color data were measured using a PhotoResearch PR-670 Colorimeter with a 10° standard observer angle and a measurement range of 360 to 860 nm in 1 nm intervals. A black box was used to house the sample and colorimeter lens while a D65 standard illuminant lamp was used to light the inside of the box. A calibrated 1/8° aperture MS-5X zoom lens was used to focus on the individual threads of the woven mesh (40 μm diameter for metal thread, 100 μm diameter fiber bundles for spandex; lens is capable of focusing on a square with a 35 μm edge). Electron microscopy was performed using an AMRAY 1810 SEM and IXRF Systems Inc. 500 Digital Processing. Image analysis was performed by ImageJ software, freely available from NIH (rsbweb.nih.gov/ij/).

Conductivity Measurements. A Keithley 224 Programmable Current Source and a 196 System DMM were used for conductivity measurements. A four-line probe was used with varying applied currents, averaged over 10 values. Three samples for each material (soaked spandex and steel mesh) were also averaged. Thicknesses were measured with a caliper.

Acknowledgment. The authors thank ITP, GmbH, for financial support of this work.

Supporting Information Available: Images of metal mesh junctions under a microscope, SEM imagery of the PEDOT-PSS loaded spandex, and synthetic details regarding the precursor polymer and its conversion to an electrochromic. This material is available free of charge via the Internet at http://pubs.acs.org

REFERENCES AND NOTES

(1) Hansen, T. S.; West, K.; Hassager, O.; Larsen, N. B. *Adv. Funct. Mater.* **2007**, *17*, 3069–3073.
(2) Hamedi, M. *Adv. Mater.* **2008**, *20*, 1–5.
(3) De Rossi, D. *Nat. Mater.* **2007**, *6*, 328–329.
(4) Hamedi, M.; Forchheimer, R.; Inganas, O. *Nat. Mater.* **2007**, *6*, 357–362.
(5) Wallace, G. G.; Campbell, T. E.; Innis, P. C. *Fibers Polym.* **2007**, *8*, 135–142.
(6) Liang, C.; Dudney, N. J.; Howe, J. Y. *Chem. Mater.* **2009**, *2119*, 4724–4730.
(7) Srivastava, S.; Podsiadlo, P.; Critchley, K.; Zhu, J.; Qin, M.; Shim, B. S.; Kotov, N. A. *Chem. Mater.* **2009**, *21* (19), 4397–4400.
(8) Mortimer, R. J.; Graham, K. R.; Grenier, C. R. G.; Reynolds, J. R. *ACS Appl. Mater. Interfaces* **2009**, *1* (10), 2269–2276.
(9) Beaujuge, P. M.; Ellinger, S.; Reynolds, J. R. *Adv. Mater.* **2008**, *20*, 2772–2776.
(10) Gunbas, G. E.; Durmus, A.; Toppare, L. *Adv. Mater.* **2008**, *20*, 691–695.
(11) Sonmez, G.; Shen, C. K. F.; Rubin, Y.; Wudl, F. *Angew. Chem., Int. Ed.* **2004**, *43*, 1498–1502.
(12) Galand, E. M.; Mwaura, J. K.; Argun, A. A.; Abboud, A. K.; McCarley, T. D.; Reynolds, J. R. *Macromolecules* **2006**, *39*, 7286–7294.
(13) Beaujuge, P. M.; Ellinger, S.; Reynolds, J. R. *Nat. Mater.* **2008**, *7*, 795–799.

(14) Unur, E.; Beaujuge, P. M.; Ellinger, S.; Jung, J.-H.; Reynolds, J. R. *Chem. Mater.* **2009**, *21* (21), 5145–5153.

(15) Yen, H.-J.; Liou, G.-S. *Chem. Mater.* **2009**, *21* (17), 4062–4070.

(16) Arsenault, A. C.; Puzzo, D. P.; Manners, I.; Ozin, G. A. *Nat. Photonics* **2007**, *1*, 468–472.

(17) Jiang, H.; Taranekar, P.; Reynolds, J. R.; Schanze, K. S. *Angew. Chem., Int. Ed.* **2009**, *48*, 4300–4316.

(18) Steuerman, D. W.; Tseng, H.-R.; Peters, A. J.; Flood, A. H.; Jeppesen, J. O.; Nielsen, K. A.; Stoddart, J. F.; Heath, J. R. *Angew. Chem., Int. Ed.* **2004**, *43*, 6486–6491.

(19) Bokria, J. G.; Kumar, A.; Seshadri, V.; Tran, A.; Sotzing, G. A. *Adv. Mater.* **2008**, *20*, 1175–1178.

(20) Invernale, M. A.; Seshadri, V.; Mamangun, D. M. D.; Ding, Y.; Filloramo, F.; Sotzing, G. A. *Chem. Mater.* **2009**, *21* (14), 3332–3336.

(21) Jang, S. Y.; Seshadri, V.; Khil, M. S.; Kumar, A.; Marquez, M.; Mather, P. T.; Sotzing, G. A. *Adv. Mater.* **2005**, *17*, 2177–2180.

(22) Invernale, M. A.; Ding, Y.; Mamangun, D. M. D.; Yavuz, M. S.; Sotzing, G. A. *Adv. Mater.*, **2009**, in press.

(23) Hanlon, R. *Curr. Biol.* **2007**, *17*, R400–R404.

(24) Cuthill, I. C.; Stevens, M.; Sheppard, J.; Maddocks, T.; Parraga, C. A.; Troscianko, T. S. *Nature* **2005**, *434*, 72–74.

(25) Costa, J. T. *Nature* **2007**, *448*, 408.

(26) Kramer, R. M.; Crookes-Goodson, W. J.; Naik, R. R. *Nat. Mater.* **2007**, *6*, 533–538.

(27) Messenger, J. B. *Biol. Rev.* **2001**, *76*, 473–528.

(28) Pendry, J. B.; Schurig, D.; Smith, D. R. *Science* **2006**, *312*, 1780–1782.

(29) Cho, A. *Science* **2006**, *312*, 1120.

(30) Leonhardt, U. *Science* **2006**, *312*, 1777–1780.

(31) Lin, T.; Wang, X. *Int. J. Nanotechnol.* **2009**, *6*, 579–598.

(32) Cheng, T.; Lin, T.; Brady, R.; Wang, X. *Fibers Polym.* **2008**, *9*, 521–526.

(33) Huang, Y.; Liang, W.; Poon, J. K. S.; Xu, Y.; Lee, R. K.; Yariv, A. *Appl. Phys. Lett.* **2006**, *88*, 181102/1–181102/3.

(34) Vasilyeva, S. V.; Unur, E.; Walczak, R. M.; Donoghue, E. P.; G.; Rinzler, A. G.; Reynolds, J. R. *ACS Appl. Mater. Interfaces* **2009**, *1* (10), 2288–2297.

(35) Argun, A. A.; Aubert, P.-H.; Thompson, B. C.; Schwendeman, I.; Gaupp, C. L.; Hwang, J.; Pinto, N. J.; Tanner, D. B.; MacDiarmid, A. G.; Reynolds, J. R. *Chem. Mater.* **2004**, *16*, 4401–4412.

(36) Subbiah, J.; Beaujuge, P. M.; Choudhury, K. R.; Ellinger, S.; Reynolds, J. R.; So, F. *ACS Appl. Mater. Interfaces* **2009**, *1* (6), 1154–1158.

(37) Mei, J.; Ogawa, K.; Kim, Y.-G.; Heston, N. C.; Arenas, D. J.; Nasrollahi, Z.; McCarley, T. D.; Tanner, D. B.; Reynolds, J. R.; Schanze, K. S. *ACS Appl. Mater. Interfaces* **2009**, *1* (1), 150–161.

(38) Argun, A. A.; Cirpan, A.; Reynolds, J. R. *Adv. Mater.* **2003**, *15*, 1338–1341.

(39) Zhang, F.; Johansson, M.; Andersson, M. R.; Hummelen, J. C.; Inganas, O. *Adv. Mater.* **2002**, *14*, 663–665.

AM900767P